
TAPPING INTO THE BLACK BOX: UNCOVERING ALIGNED REPRESENTATIONS IN PRETRAINED NEURAL NETWORKS

Maciej Satkiewicz
314 Foundation, Kraków
maciej.satkiewicz@314.foundation

ABSTRACT

In this paper we argue that ReLU networks learn an implicit linear model we can actually tap into. We describe that alleged model formally and show that we can approximately pull its decision boundary back to the input space with certain simple modification to the backward pass. The resulting gradients (called *excitation pullbacks*) reveal high-resolution input- and target-specific features of remarkable perceptual alignment on a number of popular ImageNet-pretrained deep architectures. This strongly suggests that neural networks do, in fact, rely on learned interpretable patterns that can be recovered after training. Thus, our findings may have profound implications for knowledge discovery and the development of dependable artificial systems.

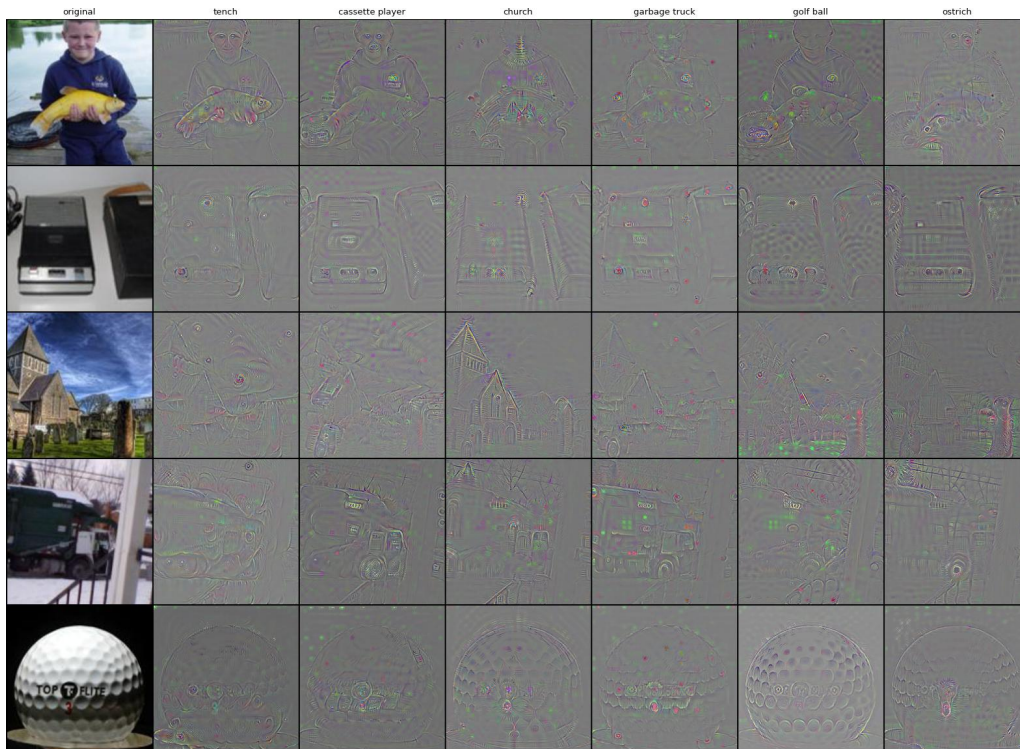


Figure 1: A rudimentary 5-step pixel-space gradient ascent guided by excitation pullbacks for pretrained ResNet50. Each cell shows the difference between the perturbed and clean image, targeting the class in the column. Diagonal: original class; off-diagonal: counterfactuals. Last column: randomly selected extra label. See Section 5 for details.

1 Introduction

This work investigates gradient-based explanations in ReLU networks, with a focus on convolutional architectures commonly used in computer vision. While our empirical results and theoretical developments concentrate on standard ReLU networks trained on image classification tasks, the core arguments are sufficiently general to apply - with the appropriate modifications - to other activation functions and modalities.

We introduce a simple but effective method for interpreting neural predictions via *excitation pullbacks*, which isolate the robust informative signal in neural activations from the noise introduced by local data peculiarities. We motivate this idea extensively and demonstrate its empirical effectiveness on the following ImageNet-pretrained ReLU models: ResNet50 [He et al., 2015], VGG11_BN [Simonyan and Zisserman, 2015], and DenseNet121 [Huang et al., 2018]. These specific architectures were chosen for reasons detailed in Section 5. We also give compelling theoretical arguments backing the claim that excitation pullbacks are indeed faithful local approximations of the network’s decision boundary. In particular, we hypothesize that they reveal a simpler linear model approximated by the trained network, encoded in the pre-activation patterns.

The paper outline is as follows:

- Section 2 introduces necessary notions and notational conventions; in particular, the gating function and gating-induced pullbacks are described;
- Section 3 defines tensor field pullbacks and shows that neural networks are linear in their path space;
- Section 4 defines excitation pullbacks and postulates that they approximate the decision boundary of an implicit kernel machine that is learned in the network’s pre-activation patterns;
- Section 5 shows that excitation pullbacks of selected architectures pretrained on the ImageNet are perceptually aligned and can be used to produce faithful and meaningful local feature accentuations by just a few steps of gradient ascent along their directions;
- Section 6 describes the related works, indicates a possible biological feasibility of presented methods and discusses their limitations.

This paper thus bridges practical gradient visualization with theoretical insights into neural function, suggesting a path toward more transparent and robust deep models.

2 Preliminaries and notational conventions

This section establishes important notions and conventions used throughout the rest of the paper.

2.1 ReLU networks

Let M be a feedforward ReLU network with parameters $\theta \in \mathbb{R}^{d_{net}}$, expressible as a composition of affine transformations and pointwise ReLU nonlinearities.¹ Let L denote the number of layers, and let d_ℓ be the width of the ℓ -th layer, with d_0 denoting the input dimension. Let x_0 denote the identity function on \mathbb{R}^{d_0} , i.e. $x_0(x) := x$. The network applies the following operations:

$$z_\ell = W_\ell x_{\ell-1} + b_\ell, \quad x_\ell = \text{ReLU}(z_\ell), \quad \text{for } \ell = 1, \dots, L$$

where $W_\ell \in \mathbb{R}^{d_\ell \times d_{\ell-1}}$, $b_\ell \in \mathbb{R}^{d_\ell}$, and $\text{ReLU}(z) = \max(0, z)$ is applied element-wise. We define the overall network function $M : \mathbb{R}^{d_0} \rightarrow \mathbb{R}^{d_L}$ by the recursive application of the layers, i.e.,

$$M(x_0) := x_L$$

In this paper we’ll treat M as backbone for some linear model, i.e. x_L represents a penultimate layer in some chosen architecture. Specifically, we’ll consider $f : \mathbb{R}^{d_0} \rightarrow \mathbb{R}$ defined by:

$$f_c := y_c^\top M$$

where y_c is a trainable set of weights $y_c \in \mathbb{R}^{d_L}$ (a neuron in the network’s head) and y_c^\top is it’s corresponding covector, i.e. the linear action of y_c on \mathbb{R}^{d_L} by the dot product: $y_c^\top x = \langle y_c, x \rangle$. Standard classification network with C classes has C corresponding vectors y_c . We will skip the lower index c assuming that it’s fixed.

¹we omit max-pooling layers from the analysis to improve clarity, while noting that similar arguments are likely to apply due to the structural similarity between max-pooling and ReLU; see Section 5.3.

Tapping into the black box

For notational brevity, we consider augmented matrices and vectors where the bias term is incorporated by appending a 1 to the end of the input vector. Specifically, we define the augmented input and weight matrix as

$$\tilde{x}_{\ell-1} = \begin{bmatrix} x_{\ell-1} \\ 1 \end{bmatrix} \in \mathbb{R}^{d_{\ell-1}+1}, \quad \tilde{W}_\ell = \begin{bmatrix} W_\ell & b_\ell \\ 0 & 1 \end{bmatrix} \in \mathbb{R}^{(d_\ell+1) \times (d_{\ell-1}+1)}$$

Then, the augmented pre-activation vector is given by

$$\tilde{z}_\ell = \tilde{W}_\ell \tilde{x}_{\ell-1}$$

Conventions

Throughout the paper, we will often abuse notation by omitting the tilde and the explicit increase of dimension, writing simply

$$z_\ell = W_\ell x_{\ell-1}$$

with the understanding that the bias is included in the matrix W_ℓ and the input vector $x_{\ell-1}$. We will occasionally write $\mathbb{R}^{d_0^*} \subset \mathbb{R}^{d_0}$ to denote the true input space (without the implicitly added coordinate). Notice that, by construction, the $\mathbb{R}^{d_0^*}$ remains the actual domain of f .

2.2 Gating representation of ReLU networks

In ReLU networks, each activation can be equivalently viewed as a gating mechanism applied to the pre-activations. Specifically, for every layer $\ell \in \{1, \dots, L\}$, the activation function

$$x_\ell = \text{ReLU}(z_\ell)$$

can be rewritten as

$$x_\ell = g_\ell \odot z_\ell$$

where $g_\ell \in \{0, 1\}^{d_\ell}$ is a binary gating vector defined by

$$g_\ell[i] = \begin{cases} 1 & \text{if } z_\ell[i] > 0, \\ 0 & \text{otherwise.} \end{cases}$$

Since z_ℓ is itself a function of the input x_0 , we may define a *gating* function

$$G : \mathbb{R}^{d_0} \rightarrow \prod_{\ell=1}^L \{0, 1\}^{d_\ell}, \quad G(x) := (g_1, \dots, g_L) \quad (1)$$

Let $G_\ell(x) = \text{diag}(g_\ell) \in \mathbb{R}^{d_\ell \times d_\ell}$ denote the diagonal matrix whose diagonal entries are given by g_ℓ . Then, the network output $M(x) = x_L$ can be written as a product of (augmented) weight matrices interleaved with input-dependent diagonal matrices:

$$M(x) = G_L(x)W_L G_{L-1}(x)W_{L-1} \cdots G_1(x)W_1 x$$

where each W_ℓ includes the bias terms via the convention introduced earlier.

This representation makes the piecewise-linear structure of ReLU networks explicit: for a fixed input x , the gating pattern $(g_1, \dots, g_L) \in \prod_{\ell=1}^L \mathbb{R}^{d_\ell}$ determines a purely linear computation.

Similarly, let's define the *pre-activation function* as:

$$Z : \mathbb{R}^{d_0} \rightarrow \prod_{\ell=1}^L \mathbb{R}^{d_\ell}, \quad Z(x) := (z_1, \dots, z_L) \quad (2)$$

i.e. the concatenation of all pre-activations of $M(x)$.

2.3 Gating-induced networks

More generally, given any gating function:

$$\Lambda : \mathbb{R}^{d_0} \rightarrow \prod_{\ell=1}^L [0, 1]^{d_\ell}, \quad \Lambda := (\lambda_1, \dots, \lambda_L), \quad \lambda_\ell : \mathbb{R}^{d_0} \rightarrow [0, 1]^{d_\ell} \quad (3)$$

we can define the Λ -induced network as

$$M_\Lambda(x) := \Lambda_L(x)W_L\Lambda_{L-1}(x)W_{L-1} \cdots \Lambda_1(x)W_1x \quad (4)$$

where $\Lambda_\ell(x) = \text{diag}(\lambda_\ell(x)) \in \mathbb{R}^{d_\ell \times d_\ell}$ is the diagonal matrix formed from the ℓ -th component λ_ℓ of $\Lambda(x)$. In particular, M is G -induced, i.e. $M = M_G$. Note that M_Λ implicitly depends on the network parameters θ .

We can also define the matrix field $\vec{M}_\Lambda : \mathbb{R}^{d_0} \rightarrow \mathbb{R}^{d_L} \times \mathbb{R}^{d_0}$ by:

$$\vec{M}_\Lambda(x) := \Lambda_L(x)W_L\Lambda_{L-1}(x)W_{L-1} \cdots \Lambda_1(x)W_1 \quad (5)$$

so that $M_\Lambda(x) = \vec{M}_\Lambda(x)x$. We set $f_\Lambda := y^\top M_\Lambda$ and therefore $f = f_G$.

2.4 Pullbacks and vector fields

Note: the symbols in this subsection 2.4 are unrelated to the rest of the section 2.

Let $f : \mathbb{R}^n \rightarrow \mathbb{R}$ be a scalar-valued function, and let $\phi : \mathbb{R}^{d_0} \rightarrow \mathbb{R}^n$ be a map. The *pullback* of f through ϕ , denoted ϕ^*f , is defined as the composition

$$\phi^*f := f \circ \phi$$

which is a function $\phi^*f : \mathbb{R}^{d_0} \rightarrow \mathbb{R}$ given explicitly by

$$(\phi^*f)(x) = f(\phi(x))$$

This construction allows us to view f as a scalar function defined directly on the domain \mathbb{R}^{d_0} (through the action of ϕ).

Convention

Whenever a piecewise continuous vector field $v : \mathbb{R}^{d_0} \rightarrow \mathbb{R}^{d_0}$ satisfies

$$\langle v(x), x \rangle = v^\top(x)x = f(\phi(x)) = (\phi^*f)(x)$$

we will refer both to v and its corresponding covector field $v^\top : \mathbb{R}^{d_0} \rightarrow (\mathbb{R}^{d_0})^*$ as pullbacks (of f through ϕ).

2.5 Gating-induced pullbacks

We can pull the linear map $y^\top : \mathbb{R}^{d_L} \rightarrow \mathbb{R}$ back to the input space \mathbb{R}^{d_0} through M_Λ , generating the following covector field over \mathbb{R}^{d_0} :

$$v_\Lambda^\top := y^\top \vec{M}_\Lambda$$

We will call both v_Λ^\top and the corresponding vector field v_Λ a Λ -pullback. In particular, we have:

$$v_G^\top = y^\top \vec{M}_G \quad (6)$$

Now, the following sequence of equations can be easily verified:

$$f_\Lambda(x) = y^\top M_\Lambda(x) = y^\top \vec{M}_\Lambda(x)x = v_\Lambda^\top(x)x = \langle v_\Lambda(x), x \rangle \quad (7)$$

This means that f_Λ is represented by its Λ -pullback v_Λ .

Now, since f is locally affine in $\mathbb{R}^{d_0^*}$ (see Section 2.1), then:

$$\nabla f = \nabla f_G = (y^\top \vec{M}_G)|_{\mathbb{R}^{d_0^*}} = (v_G^\top)|_{\mathbb{R}^{d_0^*}} \quad (8)$$

This means that $v_G|_{\mathbb{R}^{d_0^*}}$ can be easily computed as the network's gradient.

Note 2.1

The pullback representation is important for explainability as it expresses the network action as a dot product with a well-understood entity, i.e. an input-space vector (field).

2.6 Training dynamics

Network parameters θ and u change during training. We index time steps by $t \in \{0, \dots, T\}$, where $t = 0$ denotes the initialization and $t = T$ corresponds to the final state of training. Whenever an upper index (t) appears, it indicates the value of the corresponding object at training step t , for example $(y^{(t)}, \theta^{(t)})$ denotes the network parameters and $G^{(t)}$ denotes the gating function induced by $M^{(t)}$. For notational brevity, we omit the index $t = T$ when referring to the final trained model.

3 Neural networks are linear in their path space

3.1 Network action as atom filtering

Let's dive deeper into the structure of M . Fix a hidden neuron $u_\ell[i]$, i.e. the one corresponding to the i -th output in the ℓ -th layer of M . Due to the compositional nature of the network, we can define the pullback $v_\Lambda|_{(\ell,i)}$ of $u_\ell[i]$ in the same way we did for y - just consider the appropriate subnetwork below $u_\ell[i]$ as the backbone. Moreover, the full-network pullback v_Λ can be expressed as a weighted sum of the pullbacks of neurons from previous layers, for example:

$$v_\Lambda = \sum_{i=1}^{d_L} y[i] \cdot \lambda_L[i] \cdot v_\Lambda|_{(L,i)}$$

i.e. v_Λ is a weighted sum of layer- L pullbacks. This means that neurons in layer L contribute particular directions $v_\Lambda|_{(\ell,i)}$ to the full pullback v_Λ , weighted by $\lambda_L[i_L]$.

We can also express v_Λ as the weighted sum of first-layer pullbacks:

$$v_\Lambda = \sum_{(i_1, i_2, \dots, i_L)} y[i_L] \cdot \lambda_L[i_L] \cdot W_L[i_L, i_{L-1}] \cdots \lambda_2[i_2] \cdot W_2[i_2, i_1] \cdot \lambda_1[i_1] \cdot v_\Lambda|_{(1, i_1)}$$

Where (i_1, \dots, i_L) is the *path* through layers $1, \dots, L$, i.e. the selection of indices $i_\ell \in \{1, \dots, d_\ell\}$. Now rearrange the factors:

$$v_\Lambda = \sum_{(i_1, i_2, \dots, i_L)} \left(\prod_{\ell=1}^L \lambda_\ell[i_\ell] \right) \left(y[i_L] \prod_{\ell=2}^L W_\ell[i_\ell, i_{\ell-1}] \right) \cdot v_\Lambda|_{(1, i_1)}$$

Notice that $v_G|_{(1, i_1)} = (W_1[i_1])^\top \in \mathbb{R}^{d_0}$, i.e. it's a i_1 -th row of W_1 , so we have:

$$v_\Lambda = \sum_{(i_1, i_2, \dots, i_L)} \left(\prod_{\ell=1}^L \lambda_\ell[i_\ell] \right) \left(y[i_L] \prod_{\ell=2}^L W_\ell[i_\ell, i_{\ell-1}] \right) \cdot (W_1[i_1])^\top \tag{9}$$

Let $\mathcal{P}_k = \{(p_k, \dots, p_L) : p_\ell \in \{k, \dots, d_\ell\}\}$ denote the set of all paths through layers k, \dots, L , fix $p = (p_1, \dots, p_L)$, i.e. $p \in \mathcal{P}_1$ and define the *path activity* function $\Lambda^p : \mathbb{R}^{d_0} \rightarrow [0, 1]$ as:

$$\Lambda^p := \prod_{\ell=1}^L \lambda_\ell[p_\ell] \tag{10}$$

$$\tag{11}$$

Tapping into the black box

We may now rewrite the Equation 9 as:

$$v_\Lambda(x) = \sum_{p \in \mathcal{P}_1} \Lambda^p(x) \cdot \left(y[p_L] \prod_{l=2}^L W_\ell[p_\ell, p_{\ell-1}] \right) (W_1[p_1])^\top \quad (12)$$

Note 3.1

Equation 12 expresses v_Λ as a weighted sum of constant vector fields (we may call them *atoms*) indexed by \mathcal{P}_1 with the only dependence on x being via Λ^p . In case of $\Lambda = G$ this amounts to filtering the atoms by a input-specific binary mask.

3.2 Tensor field pullbacks

Setting $P_1 = |\mathcal{P}_1| = \prod_{\ell=1}^L d_\ell$ and some enumeration of \mathcal{P}_1 we may lift Λ^p to the function $\tilde{\Lambda} : \mathbb{R}^{d_0} \rightarrow \mathbb{R}^{P_1}$ by setting:

$$\tilde{\Lambda}(x) := (\Lambda^p(x))_{p \in \mathcal{P}_1} \quad (13)$$

By construction, $\tilde{\Lambda}(x)$ can be naturally identified with the tensor product of all $\lambda_\ell(x)$:

$$\tilde{\Lambda}(x) \cong \bigotimes_{\ell=1}^L \lambda_\ell(x) \in \bigotimes_{\ell=1}^L \mathbb{R}^{d_\ell} \cong \mathbb{R}^{P_1} \quad (14)$$

hence we will call \mathbb{R}^{P_1} a *tensor product* and refer to it's elements as *tensors*. Similarly $\tilde{\Lambda}$ will be called a *tensor field* over \mathbb{R}^{d_0} .

More generally, for any piecewise continuous tensor field $\tau : \mathbb{R}^{d_0} \rightarrow [0, 1]^{P_1} \subset \mathbb{R}^{P_1}$ we can define τ -pullback $v_\tau : \mathbb{R}^{d_0} \rightarrow \mathbb{R}^{d_0}$ as the following vector field:

$$v_\tau(x) := \sum_{p \in \mathcal{P}_1} \tau_p(x) \cdot \left(y[p_L] \prod_{l=2}^L W_\ell[p_\ell, p_{\ell-1}] \right) (W_1[p_1])^\top \quad (15)$$

i.e. $v_\tau(x)$ is the sum of atoms with weights determined by the tensor $\tau(x) \in \mathbb{R}^{P_1}$. Consequently, we may define the τ -induced function $f_\tau : \mathbb{R}^{d_0} \rightarrow \mathbb{R}$ as

$$f_\tau(x) := \langle v_\tau(x), x \rangle \quad (16)$$

It's easy to see that $v_\Lambda = v_{\tilde{\Lambda}}$ and $f_\Lambda = f_{\tilde{\Lambda}}$ (by Equations 7, 12 and 13), so we may safely overload the notation.

Note 3.2

$\tilde{\Lambda}(x) \in \bigotimes_{\ell=1}^L \mathbb{R}^{d_\ell}$ is a *rank-1* (i.e. pure) tensor, while $\tau(x)$ is allowed to be any tensor.

3.3 Path space and the linear nature of ReLU networks

Consider \mathcal{P}_0 i.e. the set of paths through layers $0, \dots, L$ and $p = (p_0, p_1, \dots, p_L)$. Let $p|_k := (p_k, \dots, p_L)$, i.e. the (unique) sub-path of p starting at layer k . We will abuse the notation and write τ_p instead of $\tau_{p|_1}$. With that remark we

Tapping into the black box

can expand $f_\tau(x)$ as:

$$\begin{aligned}
 f_\tau(x) &= \langle v_\tau, x \rangle = \sum_{p \in \mathcal{P}_1} \tau_p(x) \cdot \left(y[p_L] \prod_{l=2}^L W_l[p_l, p_{l-1}] \right) \langle (W_1[p_1])^\top, x \rangle \\
 &= \sum_{p \in \mathcal{P}_1} \tau_p(x) \cdot \left(y[p_L] \prod_{l=2}^L W_l[p_l, p_{l-1}] \right) \left(\sum_{i=1}^{d_0} W_1[p_1, i] \cdot x[i] \right) \\
 &= \sum_{p \in \mathcal{P}_1} \sum_{i=1}^{d_0} \tau_p(x) \cdot x[i] \cdot \left(y[p_L] \prod_{l=2}^L W_l[p_l, p_{l-1}] \right) W_1[p_1, i] \\
 &= \sum_{p \in \mathcal{P}_0} \tau_p(x) \cdot x[p_0] \cdot \left(y[p_L] \prod_{l=1}^L W_l[p_l, p_{l-1}] \right)
 \end{aligned}$$

Again, we call \mathbb{R}^{P_0} a *tensor product* as $\mathbb{R}^{P_0} \cong \bigotimes_{\ell=0}^L \mathbb{R}^{d_\ell} \cong \left(\bigotimes_{\ell=1}^L \mathbb{R}^{d_\ell} \right) \otimes \mathbb{R}^{d_0}$. Additionally, we refer to \mathbb{R}^{P_0} as the *path space*, as this is the space of all the neural paths in the network.

Let's define $\Omega : \mathbb{R}^{d_L} \times \mathbb{R}^{d_{net}} \rightarrow \mathbb{R}^{P_0}$ as:

$$\Omega((y, M)) := (\omega_p)_{p \in \mathcal{P}_0}, \quad \text{where } \omega_p := y[p_L] \prod_{l=1}^L W_l[p_l, p_{l-1}], \quad p = (p_0, p_1, \dots, p_L) \quad (17)$$

and a τ -induced *feature function* $\phi_\tau : \mathbb{R}^{d_0} \rightarrow \mathbb{R}^{P_0}$ as:

$$\phi_\tau(x) := (\tau_p \cdot x[p_0])_{p \in \mathcal{P}_0} \cong \tau \otimes x \quad (18)$$

We may now express f_τ as a dot product in \mathbb{R}^{P_0} :

$$f_\tau(x) = \sum_{p \in \mathcal{P}_0} (\phi_\tau(x))_p \cdot \omega_p = \langle \phi_\tau(x), \omega \rangle \quad (19)$$

Observe that the dimension of \mathbb{R}^{P_0} scales multiplicatively with the network's depth and therefore, in deeper networks, it is orders of magnitude larger than the number of network parameters (which scales additively with depth). In a sense this means that neural networks, generally considered to be overparameterised models, are actually significantly underparameterised from the path space point of view.

Notice that the τ -pullback defined earlier (Equation 15) is trivially equal to the pullback of $\omega^\top : \mathbb{R}^{P_0} \rightarrow \mathbb{R}$ through the feature function $\phi_\tau : \mathbb{R}^{d_0} \rightarrow \mathbb{R}^{P_0}$, because, by Equations 16 and 19, we have:

$$\omega^\top(\phi_\tau(x)) = \langle \omega, \phi_\tau(x) \rangle = f_\tau(x) = \langle v_\tau(x), x \rangle \quad (20)$$

Note 3.3

The equation 20 explicitly disentangles network's weights from the feature function, as, by definition, ω does not depend on τ , and ϕ_τ does not depend on the network parameters (y, θ) . This disentangled view suggests that most of the network's expressive power is due to the highly non-linear gating function G , as the network acts linearly (via $\omega \in \mathbb{R}^{P_0}$) on inputs transformed by $\phi_{\tilde{G}}$. Moreover, by Equation 20, the action of ω on $\phi_{\tilde{G}}(x)$ can be directly visualised in the input space via the action of the pullback v_G on x .

Even though $\phi_{\tilde{G}^{(t)}}$ does change during training, it is significantly more stable than the direct mapping $M_G^{(t)} : x \mapsto x_L^{(t)}$, highlighting the importance of the path-representation.

4 Excitation pullback and the implicit linear model

Earlier work has demonstrated that only a small subnetwork within a larger model is responsible for most of its performance. In particular, weight pruning techniques demonstrate that many weights in trained networks can be

Tapping into the black box

removed without significantly degrading accuracy, implying the presence of sparse, efficient subnetworks within dense architectures [Han et al., 2015]. Moreover, the Lottery Ticket Hypothesis [Frankle and Carbin, 2019] posits that such performant subnetworks often emerge early during training and can be “rewound” to their initial weights to train successfully in isolation. Together, these observations motivate the idea that the gating patterns in ReLU networks may approximately stabilize early in training, and thus may carry semantically meaningful structure even before convergence. Further motivation is provided in Section 6.1.

Let $X \subset \mathbb{R}^{d_0}$ be a fixed, compact dataset (e.g. $[0, 1]^{d_0}$ in case of images) and let $g, h : \mathbb{R}^{d_0} \rightarrow \mathbb{R}^n$ be two functions. Define:

$$\rho(x) := \text{corr}(g(x), h(x))$$

where corr denotes the Pearson correlation coefficient between the vectors $g(x)$ and $h(x)$. We say that g and h are *positively correlated* (in X) if $\rho(x)$ is positive for almost every $x \in X$, with respect to the Lebesgue measure. Similarly, we’ll call the correlation **strong** if $\rho(x)$ is high (e.g., greater than 0.7, although the exact threshold is not important) almost everywhere in X . Our core hypothesis is as follows:

Hypothesis 1 (Early emergence of stable excitation patterns). *There exists a binary tensor field $\gamma : \mathbb{R}^{d_0} \rightarrow \{0, 1\}^{\mathcal{P}^1}$ and an early training time $t_\gamma \ll T$ such that for every $t > t_\gamma$, γ is positively correlated with $\tilde{G}^{(t)}$ (the gating tensor field at time t).*

Moreover, we assume that the network encodes the field γ in its pre-activations. That is, there exists a gating function $\Gamma : \mathbb{R}^{d_0} \rightarrow \prod_{\ell=1}^L [0, 1]^{d_\ell} \subset \prod_{\ell=1}^L \mathbb{R}^{d_\ell}$ such that:

- Γ is **strongly positively correlated** with the pre-activation function $Z : \mathbb{R}^{d_0} \rightarrow \prod_{\ell=1}^L \mathbb{R}^{d_\ell}$,
- the induced rank-1 tensor field $\tilde{\Gamma} : \mathbb{R}^{d_0} \rightarrow [0, 1]^{\mathcal{P}^1}$ is **strongly positively correlated** with γ .

Comments and intuition:

1. We assume that the field γ has binary weights and therefore acts as a path filter, just like \tilde{G} ; however, it is not necessarily a rank-1 tensor, unlike \tilde{G} .
2. The field $\tilde{\Gamma}$ is composed of rank-1 tensors and thus can be seen as a uniform rank-1 approximation of γ .
3. Intuitively, γ contains paths that pass through highly excited neurons (those with strong pre-activations).
4. The field $\tilde{\Gamma}$ provides a smoother approximation to γ than any hard-gated field $\tilde{G}^{(t)}$, since it performs a form of soft thresholding; in particular, it suppresses barely active paths (i.e. those passing through weakly activated neurons) and partially recovers paths that are nearly active (i.e. those interrupted by a single weak neuron, but otherwise strong). This makes v_Γ less sensitive to hyper-local noise across linear regions when compared with v_G and more aligned with the coarser structure of the decision boundary.
5. The function Γ can be approximated as $\sigma \circ Z$, where σ is a sigmoid-like nonlinearity applied element-wise, e.g. sigmoid, softsign (with properly adjusted range), normal cumulative distribution function (normal CDF), etc. In general, σ should be neuron-specific or at least layer-specific, since it depends on the pre-activation distribution, which may be different for each neuron. In practice, thanks to the BatchNorm layers [Ioffe and Szegedy, 2015], a shared σ across all neurons often yields good empirical results (even though BatchNorm still differentiates between the neuron distributions via its `affine` parameters).
6. $\tilde{\Gamma}$ approximates the *direction* of γ (in the sense of cosine similarity) in $\mathbb{R}^{\mathcal{P}^1}$, rather than its exact L_2 -magnitude, since $\tilde{\Gamma}_p \ll 1$ for most paths p .

We refer to Γ as the *excitation function* of the network and to v_Γ as the *excitation pullback*.

Note 4.1

If the Hypothesis 1 holds, then, starting from time t_γ , the training dynamics of the network closely resembles the dynamics of a linear model f_γ with a fixed feature map ϕ_γ (see Equation 18), i.e. a kernel machine operating under the feature noise introduced by $\phi_{\tilde{G}^{(t)}}$. In particular, the decision boundary of that implicit linear model f_γ can be closely approximated by the decision boundary of f_Γ , the latter being directly visualizable by the excitation pullback v_Γ (see Section 5).

Thus, the postulated $\gamma(x)$, potentially being a higher-rank tensor, would grasp the essence of what stays *the same* across different rank-1 neural responses $G^{(t)}(x)$ to the same input stimuli x at time t during network training.

5 Empirical validation

The goal of this section is to validate Hypothesis 1 empirically. In particular, if excitation pullbacks indeed approximate the decision boundary of a more regular linear model, then they should be better aligned with the data manifold, which should lead to better perceptual alignment. Moreover, we’d expect the excitation pullback to be highly robust to the choice of σ across neurons, layers, and even architectures. This is because we’re interested in approximating the *direction* of γ (not its exact value), and we assume γ to be a binary tensor in \mathbb{R}^{P_1} , so it suffices to assign consistently higher scores to non-zero coordinates, implying robustness to hyperparameter choices.

To this end, we focus on popular and representative classes of ReLU-based architectures pretrained on ImageNet and available via the `torchvision` library, such that it is straightforward to replace most or all occurrences of ReLU and MaxPool2d (see Section 5.3) layers with our alternative variants, using a single recursive function over the child modules. Based on these criteria, we selected **ResNet50**, **VGG11_BN**, and **DenseNet121**.

Notably, determining the optimal choice of σ for every neuron or layer in a given network is outside the scope of this work. Instead, we seek a single global set of hyperparameters that performs reasonably well across all layers of a given model - and ideally, across all selected architectures. Our goal is to evaluate whether the resulting excitation pullbacks indeed exhibit a substantially improved perceptual alignment compared to standard gradients.

5.1 Experimental setup

To generate visualizations, we use the `val` split of the publicly available *Imagenette* dataset [Howard, 2019], a subset of ImageNet containing 10 easily recognizable classes. To simplify presentation, we select every other class from the dataset, i.e.: *trench, cassette player, church, garbage truck, and golf ball*.

For each visualization, we construct a batch containing one random image from each of the five selected classes. We then compute *excitation pullbacks* for the classification neuron y_c corresponding to each class, producing a 5×5 grid: each row corresponds to an input image, and each column to the target class for which the pullback is computed. We also compute the pullback for a randomly selected ImageNet class (“ostrich”), shown in the last column.

We repeat the same setup, but instead of computing a single excitation pullback, we perform a rudimentary projected gradient ascent toward the logit (pre-activation) of each class, along the excitation pullback. Specifically, at each iteration we take a gradient step of L_2 -norm 20, whose direction is given by the excitation pullback. At each step we project the perturbed image on the ball of radius $\epsilon = 100$ centered at the original image. We iterate this process 10 times and plot both the final perturbed images and their differences from the originals. For contrast, we repeat the same procedure using vanilla input gradients in place of excitation pullbacks. Note that due to the choice of ϵ , the perturbations are roughly fixed after 5 iterations (see Figure 1), the other 5 serving to further refine the perturbations and make them visually clearer.

5.2 Technical details

We can easily compute the excitation pullback v_Γ by first computing the right pre-activations z_ℓ via M_G (doing the ordinary forward pass) and then multiplying ReLU gradients by $\sigma(z_\ell)$ in the backward pass, i.e. computing *surrogate gradients* for ReLU layers. This can be achieved in PyTorch [Paszke et al., 2019] by defining the appropriate `torch.autograd.Function`, see Listing 1. Alternatively, the more flexible Forward Gradient Injection can be used [Otte, 2024].

In the experiments we use a fixed σ for all layers in all the networks, but ideally σ could be adjusted for every hidden neuron separately, based on the neuron pre-activation distribution. We’ve observed that different choices of σ produced similarly-looking pullback visualizations as long as the overall sigmoidal shape of the σ function remained the same. We’ve chosen $\sigma(z) = \text{sigmoid}(\frac{z}{\text{temp}})$ for `temp = 0.3` but any selection of the parameter `temp` from the approximate range `temp` $\in [0.15, 0.5]$ seemed to work quite well *across all the tested architectures*, which implies the considerable robustness of the method to the hyperparameter choice. Notice that Γ approaches hard gating G as `temp` goes to zero and no gating at all as `temp` goes to infinity.

We download the pretrained weights via `torchvision.models` library. Specifically, we use `resnet50`, `vgg11_bn` and `densenet121` models with the flag `pretrained=True`.² Gradients are visualised by `torchvision.utils.make_grid(scale_each=True)`. We perform the gradient ascent with images rescaled to the $[-1, 1]$ range (and then appropriately normalized before feeding to the model). We seed the dataloader with `torch.Generator().manual_seed(314)`.

²see Section 6.3 for more context.

5.3 Excitation pullbacks via MaxPool2d layer

Most convolutional architectures use spatial non-linearities in the form of MaxPool2d layers which can be viewed as a generalization of ReLU, i.e. $\text{ReLU}(z) = \max(0, z)$ and both operations propagate gradients only through the local maxima. This motivates the application of surrogate gradients to these layers as well. Analogously to the excitation pullback modification for ReLU, we leave the forward pass of max pooling unchanged, but replace its gradient with that of a *softmax* pooling operation, using the strike-through trick. This indeed smoothens the pullbacks even further. Implementation details can be found in the Listing 2; in particular, we set the `temperature` parameter to 0.3, the same as in surrogate gradient for ReLU.

5.4 Plotting excitation pullbacks

We present the plots generated according to the procedure described in Section 5.1, i.e. Figures 2, 3 and 4. As shown in the experiments, a single choice of the function σ performs reasonably well across all considered architectures, indicating a substantial robustness of excitation pullbacks to hyperparameter selection. As noted in Section 5.2, the visualizations remain qualitatively similar across a wide range of σ choices. Moreover, excitation pullbacks tend to highlight similar features across architectures, which suggests that the models learn comparable feature representations. Finally, the structure of the excitation pullbacks intuitively reflects the internal organization of each network, reinforcing our hypothesis that they indeed faithfully capture the underlying decision process of the model.

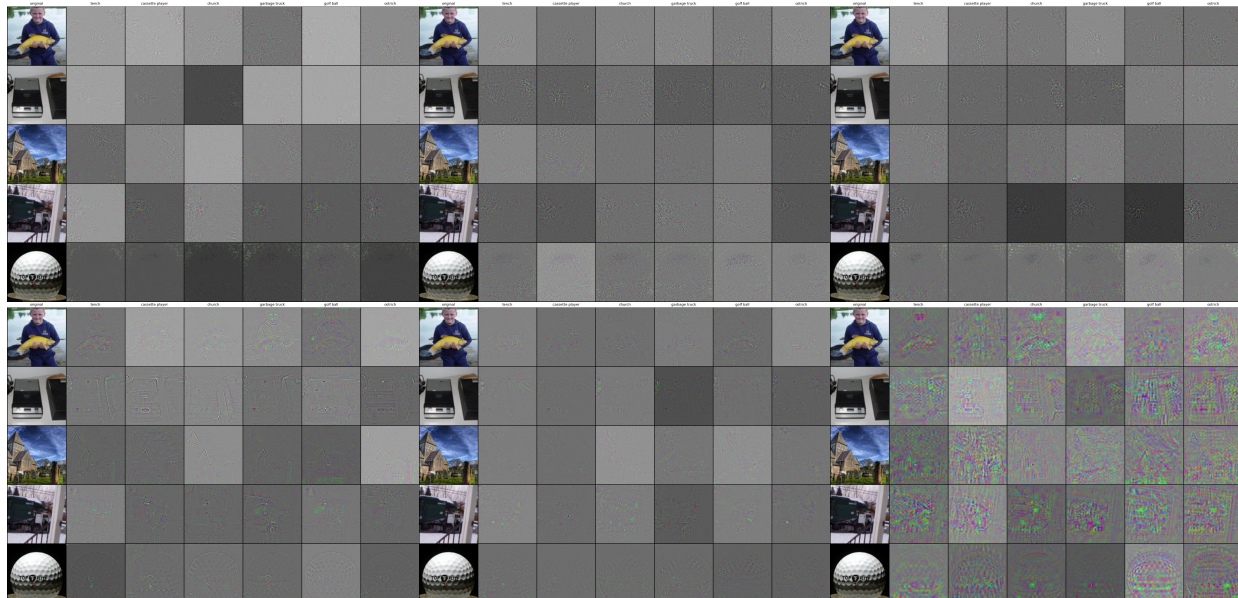


Figure 2: Top row: vanilla gradients; bottom row: excitation pullbacks. From left to right: ResNet50, VGG11_BN, DenseNet121.

6 Discussion

6.1 Related work

Similar approach to ReLU networks from the path perspective has appeared in [Yadav et al., 2024] where authors study the so called Deep Linearly Gated Networks (DLGN) in which the gating function G is computed by a parallel *linear* model M with independent set of parameters θ . The authors show that such models are considerably more interpretable than standard DNN’s and retain much of their performance. In their previous works [Lakshminarayanan and Singh, 2021] the authors define Neural Path Features (NPF) which are reminiscent of our gating functions (see Equation 3) and argue that “almost all the information learnt by a DNN with ReLU activations is stored in the gates”. They introduce Deep Gated Networks (DGN) and provide more evidence in their later work that gate adaptation is the key to generalisation [Lakshminarayanan and Singh, 2020], most notably, that “the winning lottery is in the gating pattern”, which reinforces our Hypothesis 1.

Tapping into the black box



Figure 3: Left: Image perturbations after 10-step projected gradient ascent along excitation pullbacks toward each of the classes (columns). Right: Difference between the perturbed and original images. From top to bottom: ResNet50, VGG11_BN, DenseNet121. One can clearly distinguish label-specific features highlighted by the model on every image. Compare with the same plots for vanilla gradients, Figure 4

In [Linse et al., 2024] it is shown that setting the negative slope of LeakyReLU considerably higher in the backward pass than the forward pass leads to much better aligned global feature visualisations via activation maximization, which can be directly explained by our results as LeakyReLU is equivalent to setting constant excitation function for each of the real half-lines (e.g. 1 for positive values and 0.3 for non-positive). In [Horuz et al., 2025] they generalize this idea to ReLU’s with different surrogate gradients, which is even closer to our approach, indicating that particular selection of surrogate ReLU gradient (e.g. B-SiLU) consistently improves generalization performance. Combined with our findings this leads to the open question, whether computing excitation pullbacks (instead of vanilla gradients) during training can improve generalization, and to what extent. Intuitively, one should not differentiate through the excitation gates explicitly as otherwise they may saturate and make the network overfit to the training data.

Another closely related work concerns local *feature accentuations*, [Hamblin et al., 2024] where authors obtain high-quality local feature visualizations that are specific to the seeded image and the target feature. Furthermore, they argue that these accentuations are processed by the model along it’s natural circuit. Even though the produced images are of remarkably high quality, the proposed method uses strong image regularizations during the gradient ascent (in particular, images need to be transformed to the frequency domain) and requires as much as 100 gradient steps. Furthermore, the faithfulness of the produced explanations is established intuitively, without referencing the training dynamics.

It has been observed that networks trained to be robust to adversarial perturbations yield gradients that are often aligned with human perception, a phenomenon first observed in [Tsipras et al., 2019] and then referred to as *perceptually-aligned gradients* (PAG) in [Kaur et al., 2019]. In [Srinivas et al., 2024] the authors attribute the PAG property to *off-manifold robustness*, which leads input gradients to lie approximately on the data manifold. This resonates with our observation that excitation pullback v_{Γ} provides a smoother approximation of the model’s decision boundary than the standard, hard-gated gradients (see Comments in Section 4) and therefore, by extension, may better align with the actual data manifold.

Our work suggests that even standard pretrained networks contain highly structured, semantically meaningful representations - but these get obfuscated by what we interpret as *inherent gradient noise*. This observation aligns with the broader perspective that explainability is not absent in modern networks, but merely *hidden*, and seemingly recoverable by principled methods such as ours.

6.2 On the possible biological plausibility of the implicit linear model

Intuitively, the relative stability of the gating mechanism throughout training is reminiscent of the approximately fixed synaptic connections observed in biological neural systems. In this analogy, the discrete gating pattern can be thought of as defining a persistent connectivity structure - akin to neural connections - while the excitation function describes the level of activity (excitation) of each neuron, resembling the frequency-based coding of information.

One may even venture a more speculative interpretation: the excitation pullbacks could be loosely associated with internal subjective representations, i.e. *qualia* - subjective, localized manifestations of experience that emerge from the brain activity taken as a whole - in a way similar to how excitation pullbacks emerge from the gating pattern in ReLU networks. This may open exciting direction in neuroscience and the philosophy of mind.

6.3 Limitations

Our experiments were run on pretrained `torchvision` models downloaded with the flag `pretrained=True`. This flag is now deprecated in the recent versions of the library, in particular it returns the older `ResNet50_Weights.IMAGENET1K_V1`. We’ve observed that it’s harder (but still possible) to achieve similar quality of excitation pullbacks for the more recent `ResNet50_Weights.IMAGENET1K_V2` weights, at least when using a single σ for all the neurons, which, as we’ve indicated earlier, might be an oversimplified approach. We speculate that this is because of different distribution of pre-activations in newer versions of the pretrained models.

The formal theory developed in this paper concerns specifically the ReLU networks. Intuitively, similar arguments should hold for other activation functions, in particular the the ones similar to ReLU, e.g. SiLU and GELU. Initial experiments for those architectures show promise but require certain refinement of the computation of Γ to account for the more complex gradients. However, it’s not straightforward to apply our results to attention-based models.

7 Acknowledgments

This research was supported by a private grant. The reader might find it interesting to review the [public weekly log](#) from the research.

References

- Jonathan Frankle and Michael Carbin. The lottery ticket hypothesis: Finding sparse, trainable neural networks, 2019. URL <https://arxiv.org/abs/1803.03635>.
- Chris Hamblin, Thomas Fel, Srijani Saha, Talia Konkle, and George Alvarez. Feature accentuation: Revealing 'what' features respond to in natural images, 2024. URL <https://arxiv.org/abs/2402.10039>.
- Song Han, Jeff Pool, John Tran, and William J. Dally. Learning both weights and connections for efficient neural networks, 2015. URL <https://arxiv.org/abs/1506.02626>.
- Kaiming He, Xiangyu Zhang, Shaoqing Ren, and Jian Sun. Deep residual learning for image recognition, 2015. URL <https://arxiv.org/abs/1512.03385>.
- Coşku Can Horuz, Geoffrey Kasenbacher, Saya Higuchi, Sebastian Kairat, Jendrik Stoltz, Moritz Pesl, Bernhard A. Moser, Christoph Linse, Thomas Martinetz, and Sebastian Otte. The resurrection of the relu, 2025. URL <https://arxiv.org/abs/2505.22074>.
- Jeremy Howard. Imagenette and imagewoof: Subsets of imagenet for quick experiments. <https://github.com/fastai/imagenette>, 2019. Accessed: 2025-07-21.
- Gao Huang, Zhuang Liu, Laurens van der Maaten, and Kilian Q. Weinberger. Densely connected convolutional networks, 2018. URL <https://arxiv.org/abs/1608.06993>.
- Sergey Ioffe and Christian Szegedy. Batch normalization: Accelerating deep network training by reducing internal covariate shift, 2015. URL <https://arxiv.org/abs/1502.03167>.
- Simran Kaur, Jeremy Cohen, and Zachary C. Lipton. Are perceptually-aligned gradients a general property of robust classifiers?, 2019. URL <https://arxiv.org/abs/1910.08640>.
- Chandrashekar Lakshminarayanan and Amit Vikram Singh. Deep gated networks: A framework to understand training and generalisation in deep learning, 2020. URL <https://arxiv.org/abs/2002.03996>.
- Chandrashekar Lakshminarayanan and Amit Vikram Singh. Neural path features and neural path kernel : Understanding the role of gates in deep learning, 2021. URL <https://arxiv.org/abs/2006.10529>.
- Christoph Linse, Erhardt Barth, and Thomas Martinetz. Leaky relus that differ in forward and backward pass facilitate activation maximization in deep neural networks. In *2024 International Joint Conference on Neural Networks (IJCNN)*, page 1–8. IEEE, June 2024. doi: 10.1109/ijcnn60899.2024.10650881. URL <http://dx.doi.org/10.1109/IJCNN60899.2024.10650881>.
- Sebastian Otte. Flexible and efficient surrogate gradient modeling with forward gradient injection, 2024. URL <https://arxiv.org/abs/2406.00177>.
- Adam Paszke, Sam Gross, Francisco Massa, Adam Lerer, James Bradbury, Gregory Chanan, Trevor Killeen, Zeming Lin, Natalia Gimelshein, Luca Antiga, Alban Desmaison, Andreas Köpf, Edward Yang, Zach DeVito, Martin Raison, Alykhan Tejani, Sasank Chilamkurthy, Benoit Steiner, Lu Fang, Junjie Bai, and Soumith Chintala. Pytorch: An imperative style, high-performance deep learning library, 2019. URL <https://arxiv.org/abs/1912.01703>.
- Karen Simonyan and Andrew Zisserman. Very deep convolutional networks for large-scale image recognition, 2015. URL <https://arxiv.org/abs/1409.1556>.
- Suraj Srinivas, Sebastian Bordt, and Hima Lakkaraju. Which models have perceptually-aligned gradients? an explanation via off-manifold robustness, 2024. URL <https://arxiv.org/abs/2305.19101>.
- Dimitris Tsipras, Shibani Santurkar, Logan Engstrom, Alexander Turner, and Aleksander Madry. Robustness may be at odds with accuracy, 2019. URL <https://arxiv.org/abs/1805.12152>.
- Mahesh Lorik Yadav, Harish Guruprasad Ramaswamy, and Chandrashekar Lakshminarayanan. Half-space feature learning in neural networks, 2024. URL <https://arxiv.org/abs/2404.04312>.

Listing 1: PyTorch implementation of the backward pass through ReLU

```

class TwoWayReLUFunction(torch.autograd.Function):
    @staticmethod
    def forward(ctx, z, temperature=0.3):
        ctx.save_for_backward(z)
        ctx.temperature = temperature
        return F.relu(z)

    @staticmethod
    def backward(ctx, grad_output):
        (z,) = ctx.saved_tensors
        temp = ctx.temperature

        gate = F.sigmoid(z / temp)

        return grad_output * gate, None

```

Listing 2: PyTorch implementation of the backward pass through MaxPool2d

```

import torch.nn as nn
import torch.nn.functional as F

class SoftMaxPool2d(nn.MaxPool2d):
    def __init__(self, *args, temperature=0.3, **kwargs):
        super().__init__(*args, **kwargs)
        self.temperature = temperature

    def forward(self, x):
        B, C, H, W = x.shape
        kH, kW = self.kernel_size, self.kernel_size

        # Unfold input to patches
        x_unf = F.unfold(x, kernel_size=self.kernel_size,
                        stride=self.stride, padding=self.padding)
        x_unf = x_unf.view(B, C, kH * kW, -1)

        # Softmax pooling over spatial positions
        weights = F.softmax(x_unf / self.temperature, dim=2)
        pooled = (x_unf * weights).sum(dim=2)

        # Reshape back to image
        out_H = (H + 2*self.padding - kH) // self.stride + 1
        out_W = (W + 2*self.padding - kW) // self.stride + 1
        return pooled.view(B, C, out_H, out_W)

class SurrogateSoftMaxPool2d(SoftMaxPool2d):
    def forward(self, x):
        soft = super().forward(x)
        hard = F.max_pool2d(x, self.kernel_size, self.stride,
                           self.padding, self.dilation,
                           ceil_mode=self.ceil_mode,
                           return_indices=self.return_indices)
        return hard.detach() + (soft - soft.detach())

```

Tapping into the black box



Figure 4: Left: Image perturbations after 10-step projected gradient ascent along vanilla gradients toward each of the classes (columns). Right: Difference between the perturbed and original images. From top to bottom: ResNet50, VGG11_BN, DenseNet121. The features are barely discernible. Compare with the same plots for excitation pullbacks, Figure 3